J. Fluid Mech. (1994), *vol.* 264, *pp.* 321–342

The viscous interaction between sound waves and the trailing edge of a supersonic splitter plate

By N. PEAKE

Department of Applied Mathematics and Theoretical Physics, University of Cambridge, Silver Street, Cambridge CB3 9EW, UK

(Received 21 June 1993 and in revised form 16 September 1993)

We consider the flow resulting from the interaction between the trailing edge of a supersonic splitter plate and sound waves incident on the trailing edge from upstream, as a model problem of relevance to understanding the unsteady flow in the vicinity of a supersonic jet nozzle. Morgan has previously shown that there is only one plausible solution to the outer potential-flow problem in this supersonic system, in which the vortex-sheet deflection close to the trailing edge varies linearly with the distance from the trailing edge, and that, in contrast to the subsonic version of the problem, it is not possible to construct an outer solution in which the vortex sheet leaves the plate smoothly (i.e. with zero gradient). In this paper our aim is to establish that this supersonic potential-theory solution is consistent with the equations governing the viscous flow close to the plate, and to provide a description of the nature of this inner flow, and we proceed by applying asymptotic analysis in the limit of large Reynolds number. For appropriate choices of the incident-wave amplitude and frequency, the canonical triple-deck structure at the trailing edge is realized, and the governing equations are then simplified by linearizing about the steady base flow in the lower deck; upstream of the trailing edge the unsteady flow is calculated analytically, whilst downstream a two-region parabolic scheme is employed. Our inner viscous flow is seen to match onto the outer potential-theory solution, and in particular we verify that the downstream evolution of the lower-deck flow as it emerges into the outer region corresponds exactly to the behaviour of the vortex sheet at the trailing edge in the outer flow. Once the consistency of the outer solution has been established, the dependence on the various flow parameters can be investigated, and we demonstrate in particular that significant unsteady shear-layer disturbances can be generated at the trailing edge over a wide range of values of the incidence angle, and that the amplitude of these disturbances decreases with increasing supersonic flow speed.

1. Introduction

The question of noise generation by high-speed supersonic jets has attracted increased interest in recent years, given the possible development of a second generation of civilian supersonic transport aircraft. One aspect of this problem is the interaction between the lip of the jet nozzle and acoustic waves in the flow (which might be generated by, for instance, some engine component upstream, or by the interaction of turbulence and the shocks in the jet core downstream). This is an important issue since it provides both in general an initial condition for determining the downstream

evolution of instability waves launched from the lip into large-scale coherent structures on the jet, as well as being relevant to the phenomenon of 'screech', which is thought to arise as a result of feedback between the shock cells on the jet and the nozzle lip. In this paper we shall therefore consider the unsteady flow in the close proximity of the nozzle lip, which, on the lengthscales of interest in this paper, can be represented by the trailing edge of a flat plate.

A large body of work has been completed on both the steady and the unsteady flow in the vicinity of the trailing edge of a splitter plate, concerning both the outer inviscid and inner boundary-layer regions. Considering first steady flows, Stewartson (1969) and Messiter (1970) studied the steady incompressible flow near the trailing edge of a flat plate with equal free-stream velocities on either side of the plate, and concluded that in the limit of large Reynolds number the Blasius boundary layer upstream and the Goldstein wake downstream merge in the now familiar triple-deck structure in the vicinity of the trailing edge. Subsequently Daniels has generalized Stewartson's and Messiter's approach to the cases of supersonic flow (Daniels 1974), and of unequal free-stream speeds on either side of the plate (Daniels 1977); in the particular case of stagnant flow on one side of the plate it turns out that to leading order the effects of the trailing edge are not felt on the triple-deck scale, but are localized in a much smaller region around the trailing edge. Brown & Stewartson (1970) have investigated the relationship between the steady Kutta condition and the viscous flow in the vicinity of the trailing edge of an airfoil at incidence.

Turning now to unsteady trailing-edge flows, we mention first the work of Orszag & Crow (1970), who considered the unsteady potential flow past the trailing edge of a splitter plate with incompressible uniform flow on one side and stagnant fluid on the other in the absence of external forcing, and it turns out that the unsteady flow is not uniquely specified by the solution of the potential-theory problem. By adding suitable eigenmodes of the steady system, Orszag & Crow construct three different solutions, each with a different form of vortex-sheet deflection near the trailing edge, and the selection of one particular solution from amongst these possibilities is made by the imposition of a Kutta condition expressing the coupling between the outer flow and the inner viscous region. One possibility is the imposition of what is termed a 'full Kutta condition', in which case the vortex sheet leaves the plate with zero gradient (in fact the unsteady deflection of the sheet is proportional to $x^{\frac{3}{2}}$, where x is the distance from the edge); whilst a second possibility, in which the vortex sheet leaves the trailing edge with infinite gradient (unsteady deflection proportional to $x^{\frac{1}{2}}$) is termed the 'no-Kutta-condition solution'. Orszag & Crow, however, argue in favour of what they call a 'rectified Kutta condition', in which the non-singular steady eigenfunction corresponding to a parabolic displacement of the vortex sheet is added onto the potential-theory solution in such a way that the vortex sheet bends upwards into the moving stream at all times. In order to resolve the question of the edge behaviour in Orszag & Crow's problem, Daniels (1978) has considered the structure of the boundary-layer flow in the vicinity of the trailing edge, in an attempt to match an inner solution onto the various possible outer flows, and has demonstrated that the full-Kutta-condition solution can indeed be matched consistently with a viscous flow on the triple-deck scale. Daniels also demonstrates that the no-Kutta-condition solution cannot be matched onto the boundary-layer flow for oscillations of the same amplitude as in the full-Kutta-condition solution – suggesting that such a flow would then not be sustained and that separation would occur – but that a matching could be made for much smaller amplitudes of oscillation (this matching depends on the existence of a solution of a formidable numerical problem in a small region about

the trailing edge, and remains an open question). We also mention here that the unsteady viscous flow near the trailing edge of an oscillating airfoil in an incompressible mainstream has been considered by Brown & Daniels (1975), and that the structure of this flow is in fact very similar to that found by Daniels in the splitter-plate problem. Crighton (1972*a*) has considered the compressible version of Orszag & Crow's system, and suggests that a large increase in the level of radiated sound occurs when the full Kutta condition is applied at the trailing edge; however, Howe (1978) has pointed out that this solution to the unforced problem is composed of incoming waves at infinity, and must therefore be rejected. Crighton & Leppington (1974) have developed a causal solution to the forced problem of the scattering of sound from a point source by a subsonic splitter plate; in addition, Rienstra (1981) has considered both the outer and inner problems for diffraction of acoustic waves by a trailing edge with equal free-stream velocities on either side of the plate, and again demonstrates that the application of a Kutta condition can have a significant impact on the level of aerodynamic noise generation. Reviews of the application of Kutta conditions in a wide variety of situations and of trailing-edge noise theories have been given by Crighton (1985) and Howe (1978) respectively.

Morgan (1974) has considered the potential flow corresponding to the diffraction of acoustic waves from a point source by the trailing edge of a splitter plate separating stagnant fluid from a uniform *supersonic* stream, and this can be thought of as essentially being the supersonic analogue of Orszag & Crow's problem (the problem solved by Orszag & Crow is unforced, but it turns out that it is not possible to find a supersonic attached-flow solution in the absence of external forcing). In contrast to the incompressible problem, however, there is in fact only one plausible supersonic solution, in which the vortex sheet leaves the splitter plate with a non-zero, but finite, gradient (i.e. deflection proportional to x close to the trailing edge) and in which the pressure at the trailing edge is discontinuous. It is not possible to find a potential-theory solution in which the behaviour at the trailing edge is any smoother than this by the addition of a suitable combination of steady eigenmodes, since all the appropriate eigenmodes are themselves singular at the trailing edge, as discussed by Guo (1990*a*,*b*); in particular, it is not possible to find an analogue of the subsonic full-Kutta-condition solution, in which the vortex sheet leaves the splitter plate with zero gradient. In this paper we therefore aim to establish that this single supersonic potential-theory solution can be matched consistently onto an inner viscous flow (and this is far from obvious *a priori*, given that in the incompressible problem the outer solution in which the vortex sheet fails to leave the plate with zero gradient cannot necessarily be matched onto an inner solution), and to provide a description of this inner solution.

We consider a different outer problem to the one solved formally by Morgan (1974) (which will have the advantage of yielding rather more tractable expressions for the various unsteady quantities to be calculated), and suppose that *plane waves* are incident on the trailing edge from the supersonic stream; the viscous flow in the case of waves incident from the stagnant fluid is in fact very similar. The potential-theory outer solution is outlined in § 2, and the behaviour of the unsteady flow near the trailing edge, which will be required for matching onto the inner solution, is determined. In § 3, the structure of the inner solution in the limit of large Reynolds number and for particular choices of the incident amplitude and frequency is described, and the problem of determining the flow in the vicinity of the trailing edge is seen to reduce to the solution of the unsteady boundary-layer equations in the lower deck with appropriate boundary conditions (the structure of the boundary-layer flow

turns out to be similar to that determined by Daniels 1975 for an oscillating airfoil in supersonic flow). In § 4, we simplify these equations by supposing that the unsteady viscous flow generated by the incident-wave interaction is a small perturbation to the steady base flow, allowing the lower-deck equations to be linearized; upstream of the trailing edge this linearized system can then be solved analytically, whilst downstream the solution is determined numerically using a two-region finite-difference scheme developed by Smith (1974). The numerical lower-deck solution is seen to converge to a Goldstein wake flow downstream, the centreline of which oscillates harmonically in time, and which in turn is seen to match onto the vortex-sheet deflection near the trailing edge.

2. Potential-theory solution

In this section we describe the outer potential-theory solution for our supersonic splitter-plate problem. A number of studies on related problems already exist, and in particular we mention here the work of Morgan (1974), who considers a supersonic splitter plate with a sound source at a finite distance from the plate in the stationary fluid, and Crighton (1972*a*, *b*), who considers the scattering of incident plane waves by a trailing edge with particular reference to low-Mach-number flows. The details of our analysis are in fact similar to the work described in the above, and only an outline is required here; in what follows, we shall concern ourselves with extracting closed-form expressions for the behaviour of the unsteady flow in the vicinity of the trailing edge from the potential-theory solution.

We consider a semi-infinite rigid plate lying along the negative x-axis, with uniform steady mean flow parallel to the plate in $y > 0$, and with zero mean flow in $y < 0$; the mean-flow velocity is U_∞, and we suppose for definiteness that the sound speed, c_∞, is uniform throughout the fluid – consideration of the effects of differing sound speeds in the uniform-stream and stagnant regions could easily be included (Cargill 1982). The mean-flow Mach number is simply $M = U_\infty/c_\infty$, and in our supersonic problem we have $M > 1$; we shall also suppose, again for definiteness, that $M < 2\sqrt{2}$, in which case the flow possesses the familiar Kelvin–Helmholtz instability (see for example Jones & Morgan 1973). A plane harmonic wave, with frequency ω, is incident on the plate from upstream in $y > 0$, and we suppose that the wave phase fronts make an angle θ_i with the x-axis, so that the wavenumbers associated with the x- and y-directions, k_1 and $-\gamma_1(k_1)$, are given by

$$(k_1, -\gamma_1(k_1)) = \left(\frac{k_0 \cos\theta_i}{1 + M\cos\theta_i}, \frac{-k_0 \sin\theta_i}{1 + M\cos\theta_i} \right) , \tag{2.1}$$

where $k_0 = \omega/c_\infty$. We assume that the amplitude of this incident wave is small, so that the resulting scattered field can be taken as irrotational (apart from the vortex sheet shed from the trailing edge), and the total unsteady velocity potential (i.e. the sum of incident and scattered fields) is then denoted $\varphi_{1,2}(x, y)\exp(i\omega t)$ in $y > 0$ and $y < 0$ respectively, where $\varphi_1(x, y)$ satisfies the convected form of the Helmholtz equation,

$$\left(M\frac{\partial}{\partial x} + ik_0 \right)^2 \varphi_1 - \nabla^2\varphi_1 = 0 , \tag{2.2}$$

and where φ_2 satisfies (2.2) with M set to zero. For boundary conditions we shall require that the total normal velocity on the plate is zero, that the transverse velocity of the vortex sheet is equal to the y-component of the fluid velocity on either side of

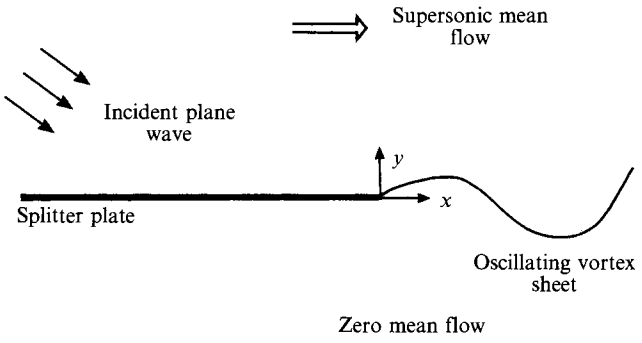

FIGURE 1. The geometry of the outer problem.

the vortex sheet, and that the pressure is continuous across the vortex sheet. We shall also require the solution to be causal, and in order to do this we deform subsequent integration contours in the way prescribed by Crighton & Leppington (1974). The system is shown in figure 1.

The solution will be completed by use of Fourier transforms, but before doing this it proves necessary to separate off explicitly the waves which are reflected from, and transmitted through, the vortex sheet, since the transforms of these components are not well-defined. This decomposition has been completed by Crighton (1972*b*), and involves the application of the boundary conditions pertaining to the vortex sheet along the entire x-axis. Once these transmitted and reflected components have been determined, we can write down expressions for the total unsteady potentials above and below the plate, and for the total unsteady displacement of the vortex sheet (denoted $\eta(x)\exp(\mathrm{i}\omega t)$), as follows:

$$\varphi_1(x,y) = I\exp(-\mathrm{i}k_1x + \mathrm{i}\gamma_1(k_1)y) + R\exp(-\mathrm{i}k_1x - \mathrm{i}\gamma_1(k_1)y) + \phi(x,y)\ , \tag{2.3}$$

$$\varphi_2(x,y) = T\exp(-\mathrm{i}k_1x + i\gamma_2(k_1)y) + \psi(x,y)\ , \tag{2.4}$$

$$\eta(x) = H\exp(-\mathrm{i}k_1x) + \xi(x)\ . \tag{2.5}$$

The functions $\phi(x,y)$, $\psi(x,y)$ and $\xi(x)$ represent the scattered potentials above and below the plate and the transverse displacement of the vortex sheet respectively, once the components corresponding to the transmission and reflection of the incident wave by the vortex sheet have been subtracted. In addition, $\gamma_2(k_1)$ corresponds to the transverse wavenumber of the transmitted wave, and can be determined by elementary methods; the definitions of $\gamma_{1,2}(k)$ are given below. The quantities R and T are related to the effective reflection and transmission coefficients of the vortex sheet, and together with H, the amplitude of the deflection of the sheet associated with the incident wave, can be found in terms of the incident amplitude I in a straightforward manner.

Now that the reflected and transmitted components have been explicitly removed, we can take Fourier transforms of $\phi(x,y)$, $\psi(x,y)$ and $\xi(x)$ with respect to x, denoted by $\Phi(k,y)$, $\Psi(k,y)$ and $\Xi(k)$ respectively, with

$$\Phi(k,y) \equiv \int_{-\infty}^{\infty} \phi(x,y)\exp(\mathrm{i}kx)\mathrm{d}x\ , \tag{2.6}$$

and the inversion contour for these transforms must be chosen in such a way as to yield a causal solution; this choice is complicated by the presence of the Kelvin–Helmholtz convective instability, and will be discussed below. It can then be shown

that

$$c_\infty G(k)\Xi(k) + \Phi^-(k,0)(k_0 - Mk) - \Psi^-(k,0)k_0 - \mathrm{i}M\phi(+0,+0) = \frac{-\mathrm{i}T\gamma_2(k_1)G(k)}{(k-k_1)k_0} \quad , \tag{2.7}$$

where

$$G(k) \equiv \frac{(k_0 - Mk)^2\gamma_2(k) + k_0^2\gamma_1(k)}{\gamma_1(k)\gamma_2(k)} \quad , \tag{2.8}$$

and where the superfixes $\pm$ indicate that the Fourier transforms have been taken over the semi-infinite intervals $x > 0$ and $x < 0$ respectively. The quantities $\gamma_{1,2}(k)$ are defined as follows:

$$\gamma_1(k) = \left((k_0 - Mk)^2 - k^2\right)^{\frac{1}{2}} \quad , \tag{2.9}$$

with a branch cut joining the two branch points and with γ_1 taking negative real values as $k \to \infty$ along the positive real axis;

$$\gamma_2(k) = \left(k_0^2 - k^2\right)^{\frac{1}{2}} \quad , \tag{2.10}$$

with branch cuts emanating from $\pm k_0$ and connecting the branch points to infinity through the lower and upper halves of the complex k-plane respectively, and with $\gamma_2(k)$ taking negative imaginary values as $k \to \infty$ along the real axis. The branch cuts are shown in figure 2. As well as these branch points, it turns out that the various Fourier transforms possess poles at the zeros of $G(k)$, and Jones & Morgan (1973) have shown that there are in fact two such poles and that, for $M < 2\sqrt{2}$ and real ω, they form the complex-conjugate pair u_0, u_0^* with $\mathrm{Im}(u_0) > 0$; the contribution from the pole $k = u_0$ corresponds to the Kelvin–Helmholtz mode (for $M > 2\sqrt{2}$ the two poles lie on the real axis, and coalesce in the limit $M \to 2\sqrt{2}$). In order to ensure that our solution is causal we follow Crighton & Leppington (1974), who considered the scattering of sound from a point source above a subsonic splitter plate. Their approach involves first solving the problem for complex ω with argument close to $-\pi/2$, and then determining the solution in the limit of the imaginary part of ω approaching zero through negative values by analytic continuation. In this way, they demonstrate that the inversion contour must be deformed to lie above both the poles at $k = u_0$ and at $k = u_0^*$.

Once the appropriate deformation of the inversion contour in the complex k-plane has been made, the solution can be completed by use of the Wiener–Hopf technique (Noble 1958), and we note first that the various transforms are analytic in the thin strip centred on the deformed inversion contour, as shown in figure 2 – the overlapping half-planes $R^\pm$ are also shown in figure 2 (here ω possesses a small negative imaginary part, which is set to zero at the end of the analysis). The most important step is to make a multiplicative factorization of $G(k)$ in the form $G(k) = G^+(k)G^-(k)$, in which $G^\pm(k)$ are analytic, non-zero and possess algebraic behaviour at infinity in $R^\pm$ respectively. This factorization has been completed by Morgan (1974), and is stated in Appendix A for completeness. Equation (2.7) can then be rewritten in a form in which the left-hand side is analytic in R^+ and the right-hand side is analytic in R^-, thereby providing the analytic continuation of a function, $E(k)$ say, from the strip $R^+ \cap R^-$ into the entire complex plane (it should be noted that the point $k = k_1$ lies in R^+). The usual Wiener–Hopf arguments can then be used to show that $E(k) \equiv 0$, yielding two equations from equation (2.7), and thereby yielding expressions for the unknown Fourier transforms of the velocity potentials and the vortex-sheet deflection. The choice $E(k) \neq 0$ would yield a solution in which the vortex sheet is not attached

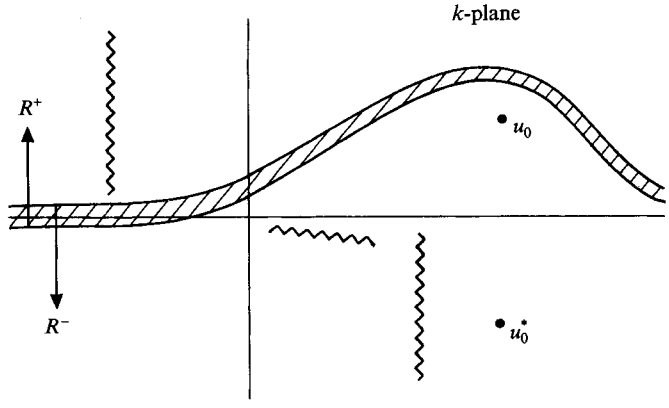

FIGURE 2. The complex k-plane employed in the solution of the outer potential-theory problem, including the branch cuts and the two zeros of $G(k)$. The overlapping half-planes R^+ and R^- lie above and below the two curved lines indicated, and their intersection, corresponding to the strip of analyticity containing the Fourier inversion contour, is hatched.

at the trailing edge, and although such an outer flow might be compatible with some inner viscous structure, we will restrict our attention here to the attached-flow case.

In principle, the scattered field throughout the fluid can now be determined by inverting the Fourier transforms derived above, but this in fact proves rather difficult, since the complicated inversion integrals cannot all be evaluated in closed form. However, for the purposes of our study it will only be necessary to determine the behaviour of the unsteady flow in the vicinity of the trailing edge, and it turns out that the relevant expressions can be derived in a relatively compact way. We consider first the unsteady deflection of the vortex sheet as it leaves the trailing edge of the plate; it can be shown from the Wiener–Hopf analysis that the Fourier transform of the modified deflection of the vortex sheet is

$$\Xi(k) = -\frac{\mathrm{i}(I-R)\gamma_1(k_1)}{c_\infty(k-k_1)(k_0-Mk_1)}\left(1-\frac{G^+(k_1)}{G^+(k)}\right), \tag{2.11}$$

and by considering the limit of $k \to \infty \in R^+$, we can determine the behaviour of $\xi(x)$ as $x \to 0+$ (see Noble 1958), and find that

$$\eta(x) \sim \frac{\mathrm{i}(I-R)\gamma_1(k_1)(M^2-1)^{\frac{1}{2}}G^+(k_1)}{M^2c_\infty(k_0-Mk_1)}x \quad \text{as} \quad x \to +0\ . \tag{2.12}$$

It can therefore be seen that the vortex sheet leaves the trailing edge with a non-zero gradient, and it should be emphasized that it is not possible to construct some alternative solution which behaves more smoothly at the trailing edge by the addition of suitable eigenmodes of the system, since, as argued by Guo (1990*a*, *b*), all the eigenmodes which could be added onto this potential solution are themselves singular, and are therefore inadmissible. This is in contrast to the subsonic version of the problem, for which it is possible to introduce an eigenmode corresponding to a parabolic deflection of the vortex sheet so as to yield a solution in which the vortex sheet leaves the trailing edge with exactly zero gradient.

In order to complete the matching with the inner viscous flow, we shall also require expressions for the unsteady pressure near the trailing edge. The unsteady pressure above and below the plate, denoted $p_{1,2}(x,y)\exp(\mathrm{i}\omega t)$, is related to the unsteady velocity potential via the linearized Bernoulli equation, and expressions

for the Fourier transforms of the pressure, $\tilde{p}_{1,2}(k, y)$, can easily be found from the Wiener–Hopf analysis. Above the plate the total unsteady pressure on $y = +0$ for $x < 0$ is

$$p_1(x, +0) = -2i\rho_\infty c_\infty I(k_0 - Mk_1) \equiv E_1 \ , \tag{2.13}$$

where ρ_∞ is the quiescent fluid density, and this result can be understood simply by noting that, since the uniform stream above the plate is supersonic, the only unsteady flow that can exist above the plate and upstream of the trailing edge consists of the incident wave plus its reflection from the plate. Alternatively, downstream of the trailing edge it is not possible to derive a closed-form expression for the pressure valid for all $x > 0$, and we proceed by determining the half-range Fourier transform of $p_1(x, y)$ over $x > 0$ and by again considering the limit of $k \to \infty \in R^+$, leading to

$$p_1(x, +0) \sim -2i\rho_\infty c_\infty (k_0 - Mk_1) \left\{ I - \frac{(I - R)\gamma_1(k_1)G^+(k_1)}{2(k_0 - Mk_1)^2} \right\} \equiv E_1 + E_2 \ \text{ as } \ x \to +0 \ . \tag{2.14}$$

By comparing equations (2.13) and (2.14) it becomes clear that the total unsteady pressure on $y = +0$ jumps across $x = 0$ by the non-zero quantity E_2, corresponding to the discontinuity across the Mach line in the supersonic main stream. Below the plate, it can be shown that the total pressure along $y = -0$ is continuous across $x = 0$, and we have that

$$p_2(-0, -0) = p_2(+0, -0) = E_1 + E_2 \ .$$

For large ω, with the amplitude of the incident pressure held fixed (i.e. vary ω but keep $I\omega$ held fixed), it is easy to see that the amplitude of the unsteady pressure in the vicinity of the trailing edge, and hence the quantities $E_{1,2}$, are independent of ω. It is also clear that there is a non-zero pressure jump across $y = 0$ for $x < 0$, corresponding to the unsteady lift on the plate.

We have therefore seen how the vortex sheet leaves the plate with unsteady displacement proportional to x, and how the unsteady pressure is discontinuous just above the trailing edge (strictly, the slip velocity on the plate close to the trailing edge is also required, but can easily be found using exactly the same arguments as described above). In the following sections we shall demonstrate that this outer flow is fully consistent with the inner viscous structure near the trailing edge (and is therefore realizable in practice), but at this point we shall anticipate this conclusion, and proceed to investigate the dependence of the vortex-sheet deflection (or equivalently the magnitude of the unsteady perturbations to the shear layer) on the Mach number M and incidence angle θ_i. In order to do this in a physically realistic way, we vary M and θ_i whilst keeping the magnitude of the incident acoustic *pressure* (which is proportional to $\omega I/(1 + M\cos\theta_i)$) held fixed, rather than simply by fixing I. In figure 3 we therefore plot the magnitude of $\eta'(0)(1 + M\cos\theta_i)/I$ against θ_i, in the range $0 < \theta_i < \theta_c$, where $\cos\theta_c = -1/(M + 1)$. It can be seen that for a given value of M the gradient of the vortex sheet at the trailing edge is non-zero, and is virtually independent of θ_i, over a wide range of acute values of θ_i, and this therefore suggests that noise generated by engine components well upstream of the nozzle can have a significant effect on the behaviour of the unsteady flow near the nozzle lip. This deflection decreases sharply for $\theta_i \geqslant \pi/2$, however, and this is hardly surprising since much of the acoustic energy generated by a source directly above or downstream of the trailing edge would be convected further downstream by the supersonic mean flow and would not interact with the trailing edge. The critical value $\theta_i = \theta_c$ corresponds to a non-uniformity in the outer solution caused by the coalescence of the branch

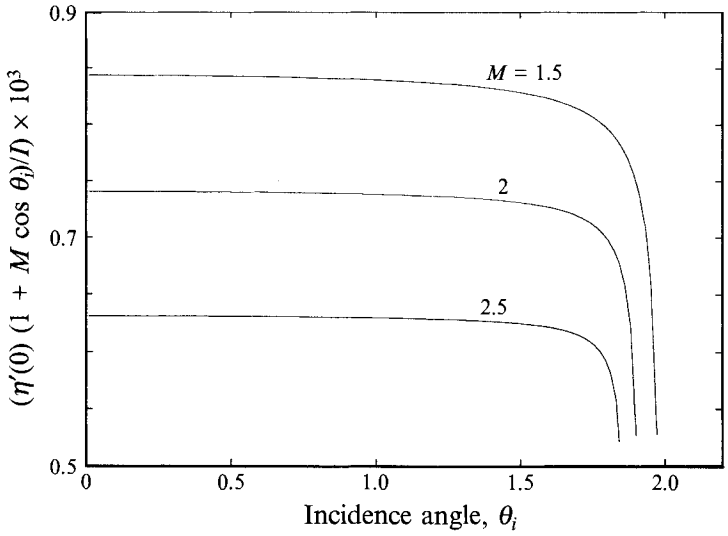

FIGURE 3. The normalized gradient of the vortex sheet in the outer potential flow at the trailing edge, $\eta'(0)(1 + M\cos\theta_i)/I$, for incidence angle, θ_i, and for various values of the mean-flow Mach number M. Here, we have taken $\omega = 100$ Hz and $c_0 = 340\ \mathrm{m\,s^{-1}}$.

point at $k = -k_0$ and the pole at $k = k_1$. Modification of the outer solution to account for this would be possible, but need not be attempted here; for $\theta_i > \theta_c$ the vortex-sheet deflection will be negligible, and indeed must be identically zero once θ_i becomes sufficiently large for the direction of the incident waves to have crossed the Mach cone emanating from the trailing edge. We can also see from figure 3 that the magnitude of the vortex-sheet deflection for a given incidence angle decreases quite markedly as the free-stream Mach number is increased in the range $1 < M < 2\sqrt{2}$.

3. Viscous flow

We suppose that a Blasius boundary layer emanates from the point $x = -l$ on the upper surface of the plate, and in what follows we ignore any effects introduced by the interaction between the incident wave and the boundary layer near this point; this would not, of course, be an appropriate simplification in the case of the interaction between sound waves and a finite airfoil, in which instability waves would be launched from the leading edge, but since our aim here is to understand the influence of the trailing edge alone in the context of jet–nozzle interactions, this approach seems a reasonable one. We can therefore define a Reynolds number $Re = U_\infty l/\nu_\infty$ where ν_∞ is the fluid kinematic viscosity far from the plate, together with the small parameter $\epsilon = (Re)^{-\frac{1}{8}}$. The asymptotic analysis presented in what follows is completed in the formal limit $\epsilon \to 0$.

Before going on to consider the unsteady viscous flow resulting from the incident-wave interaction, we must first discuss the structure of the steady flow past the splitter plate in the absence of forcing. This steady flow has been considered in the case of an incompressible main stream (Daniels 1977), and it turns out that the steady solution for our supersonic flow is very similar. Upstream of the trailing edge and above the plate the steady flow comprises a conventional compressible Blasius boundary layer, which merges at the trailing edge with the downstream Goldstein wake. The most significant feature of the steady problem, however, is the fact that in the outer region

of the flow (i.e. where $x, y = O(1)$) the $O(\epsilon^4)$ perturbation to the pressure due to the presence of the trailing edge is non-singular at the trailing edge. This can easily be seen by writing the pressure in the outer flow in the form $p_\infty + \epsilon^4 p_1 + \ldots$, and noting that in the stagnant fluid below the plate $p_1 \equiv 0$, whilst above the plate p_1 is a solution of the wave equation. By continuity of pressure across the wake, this means that $p_1(x, 0+) = 0$ for $x > 0$, and combining this with the fact that in the limit $y \to +0$ the $O(\epsilon^4)$ normal velocity in the outer region must match with the Blasius flow for $x < 0$, it is easy to show that p_1 is non-singular at the origin; the argument follows in exactly the same way as in Daniels (1977), except that in the incompressible case p_1 is of course a solution of Laplace's equation instead of the wave equation. The transition between the Blasius boundary layer and the Goldstein wake is therefore a particularly smooth one, and to leading order the steady flow does not possess any triple-deck structure, in contrast to the case of a trailing edge with non-zero mean flow on both sides (Stewartson 1969; Daniels 1974), where the singularity in the outer pressure perturbation is resolved on the triple-deck scale. In our problem, the effects of the presence of the trailing edge on the steady flow are restricted to a very small region about the trailing edge with extent $O(\epsilon^6)$, as shown by Daniels (1977) in the incompressible case. The important implication is that on the triple-deck scale the steady flow is exactly the Blasius boundary layer upstream of the trailing edge and the Goldstein wake downstream of the trailing edge, and this will make our subsequent linearization of the unsteady viscous flow about the steady base flow particularly straightforward.

The nature of the unsteady viscous flow is crucially dependent on the choice of the magnitude of the acoustic-wave frequency, ω, and we follow Daniels (1978) and Rienstra (1981) in taking $\omega = O(\epsilon^{-2})$. In order to obtain the canonical triple-deck structure at the trailing edge, the amplitude of the unsteady outer pressure perturbation at the trailing edge must be $O(\epsilon^2)$, and to achieve this it can be seen from equations (2.13) and (2.14) that we must choose $I = O(\epsilon^4)$ (given this choice of parameters, the slip velocities above and below the plate are also $O(\epsilon^2)$). We shall suppose that the fluid has Prandtl number unity and that the dynamic viscosity, μ, is related to the temperature, T, via Chapman's law, i.e.

$$\mu/\mu_\infty = C(T/T_\infty) \text{ with } C = (\mu_w T_\infty/\mu_\infty T_w) \ , \tag{3.1}$$

where μ_w and T_w are the viscosity and temperature at the wall.

Turning now to the unsteady viscous flow, the compressible-boundary-layer equations are cast into a particularly simple form using the Howarth–Dorodnitsyn transformation described by Stewartson (1964). On the upper surface of the plate and for $x = O(1)$ the viscous flow in the presence of the incident wave is given by the sum of the steady component corresponding to the Blasius boundary layer (thickness $O(\epsilon^4)$) and an unsteady term; over most of the boundary layer the latter is simply equal to the outer potential-flow slip velocity but is decelerated to zero in a thin Stokes layers (thickness $O(\epsilon^5)$) on the plate surface. On the lower side of the plate there is of course no steady Blasius flow, and the leading-order contribution is provided solely by the outer slip velocity, which is again decelerated to zero in a Stokes layer on the plate surface; we note that the steady flow below the plate is not identically zero, since, as discussed by Daniels (1977), there is a region of back flow, but this is sufficiently weak not to affect the unsteady solution to leading order. In the limit of $x \to -0$ the boundary layer is matched directly with a triple-deck structure at the trailing edge, as described below; there is no need for the addition of a fore-deck, as in the case of an oscillating airfoil in subsonic flow (Brown & Daniels 1975), essentially

because the outer unsteady pressure in our supersonic problem is non-singular (but discontinuous) at the trailing edge.

In the triple-deck region the unsteady flow is very similar to that described by Daniels (1975) for the oscillating airfoil in supersonic flow, and no details of the analysis need be presented here. The unsteady triple-deck structure, which is essentially equivalent to that first found by Stewartson & Williams (1969) near separation in steady supersonic flow, has longitudinal extent $O(\epsilon^3)$ about the trailing edge, and acts to smooth out the jump in the outer unsteady pressure described by equations (2.13) and (2.14). Determination of the flow in the triple deck reduces to the solution of the equations in the lower deck, which are simplified by introduction of scaled non-dimensional variables (denoted by capital letters); the scalings are as in Daniels (1977), and we find that

$$S\frac{\partial U}{\partial T} + U\frac{\partial U}{\partial X} + V\frac{\partial U}{\partial Y} = -\frac{\partial P}{\partial X} + \frac{\partial^2 U}{\partial Y^2} \ , \tag{3.2}$$

$$\frac{\partial U}{\partial X} + \frac{\partial V}{\partial Y} = 0 \ , \tag{3.3}$$

with

$$P(X,T) = \frac{\partial A}{\partial X} + E_1' \exp(\mathrm{i}T), \quad Y > 0 \ , \tag{3.4}$$

$$P(X,T) = (E_1' + E_2') \exp(\mathrm{i}T), \quad Y < 0 \ , \tag{3.5}$$

where

$$E_{1,2}' = \frac{E_{1,2}\epsilon^{-2}}{C^{\frac{1}{4}}\lambda^{\frac{1}{2}}(M^2-1)^{-\frac{1}{4}}p_\infty} \ . \tag{3.6}$$

Here U, V are the scaled lower-deck velocity components, S is the scaled frequency and λ is the usual Blasius wall shear. In addition, we have the boundary conditions

$$U = V = 0 \quad \text{on} \quad Y = \pm 0, X < 0 \ , \tag{3.7}$$

$$U \sim Y - A \quad \text{as} \quad Y \to \infty \ , \tag{3.8}$$

$$U \sim Y \quad \text{as} \quad X \to -\infty, Y > 0 \ , \tag{3.9}$$

$$U \sim 0 \quad \text{as} \quad X \to -\infty, Y < 0 \ . \tag{3.10}$$

Above the plate, the pressure is independent of Y through the lower and middle decks and is matched onto the discontinous outer pressure through the inviscid upper deck. Below the plate, however, given the absence of mean flow, the pressure in the lower deck is exactly equal to the outer pressure given by equation (2.14), leading to the expression given in (3.5). We can therefore conclude from the relationship between the pressure and the displacement, and from the continuity of pressure across the wake, that the displacement is

$$A(X,T) = E_2' X \exp(\mathrm{i}T) + D\exp(\mathrm{i}T) \quad \text{for} \quad X > 0 \ , \tag{3.11}$$

where D is a constant to be determined later.

4. Solution of the lower-deck equations

In this section we linearize the lower-deck problem described in equations (3.2)–(3.10) by treating the unsteady flow induced by the interaction of the incident wave as a small perturbation to the steady base flow. It is again emphasized that the steady

flow in the lower deck takes a particularly simple form in our problem; to leading order the steady flow in the lower-deck region upstream of the trailing edge and above the plate is just uniform shear, whilst below the plate the steady flow arises at a higher order than the unsteady outer slip velocity and is therefore taken as zero. Downstream of the trailing edge the steady flow is given by the limiting form of the Goldstein wake flow (Stewartson 1969), and can be expressed in terms of the solution of an ordinary differential equation.

4.1. *Unsteady flow upstream of the trailing edge*

We write the lower-deck velocity in the form

$$(U(X,Y,T),V(X,Y,T)) = (Y+\bar{U}(X,Y)\exp(\mathrm{i}T),\bar{V}(X,Y)\exp(\mathrm{i}T)) \ , \tag{4.1}$$

where $\bar{U}$ and $\bar{V}$ represent the unsteady components, with $|\bar{U}|,|\bar{V}| \ll 1$; in addition, we have $A(X,T) = \bar{A}(X)\exp(\mathrm{i}T)$ for all X. By substituting (4.1) into the lower deck equations and neglecting quadratic terms, it can be seen that above the plate and for $X<0$

$$\mathrm{i}S\bar{U} + Y\frac{\partial \bar{U}}{\partial X} + \bar{V} = -\frac{\mathrm{d}^2\bar{A}}{\mathrm{d}X^2} + \frac{\partial^2 \bar{U}}{\partial Y^2} \ , \tag{4.2}$$

$$\frac{\partial \bar{U}}{\partial X} + \frac{\partial \bar{V}}{\partial Y} = 0 \ , \tag{4.3}$$

subject to the boundary conditions

$$\frac{\mathrm{d}^2\bar{A}}{\mathrm{d}X^2} = \frac{\partial^2\bar{U}}{\partial Y^2}(X,0) \quad \text{for} \quad X<0 \ , \tag{4.4}$$

$$\bar{U}(X,Y) \sim -\bar{A}(X) \quad \text{as} \quad Y \to \infty \ , \tag{4.5}$$

$$\bar{U}(X,Y) \sim 0 \quad \text{as} \quad X \to -\infty \ , \tag{4.6}$$

where condition (4.4) has been derived by substituting the no-slip condition into (4.2). This linear system can be solved analytically, either by use of the Wiener–Hopf technique, as is done by Brown & Daniels (1975) for an oscillating airfoil in subsonic flow, or simply by supposing that the X dependence of the solution takes the form of a simple exponential in $X<0$, as is done by Daniels (1975) for an oscillating airfoil in supersonic flow and by Stewartson & Williams (1969) in their original supersonic triple-deck analysis. We begin by defining the kernel function, $\mathscr{K}(k,Y)$, by

$$\mathscr{K}(k,Y) = -\frac{1}{k^2} + \frac{\displaystyle\int_Y^\infty \mathrm{Ai}\left([(k+\mathrm{i}\delta)\exp(-\mathrm{i}\pi/2)]^{\frac{1}{3}}(t-S/k)\right)\mathrm{d}t}{[(k+\mathrm{i}\delta)\exp(-\mathrm{i}\pi/2)]^{\frac{1}{3}}\mathrm{Ai}'(y_0)} \ , \tag{4.7}$$

where

$$y_0 = [(k+\mathrm{i}\delta)\exp(-\mathrm{i}\pi/2)]^{\frac{1}{3}}(-S/k) \ , \tag{4.8}$$

and where δ is a small positive parameter which has been introduced to facilitate the definition of the third root – we suppose that there is a branch cut in the lower half of the k-plane emanating from $k=-\mathrm{i}\delta$ and running parallel to the negative imaginary axis, and that $(k+\mathrm{i}\delta)^{\frac{1}{3}}$ takes positive real values as $k \to \infty$ on the real axis. Whichever of the two methods of solution is used, the key step is now to determine the roots of the equation

$$\mathscr{K}(k,0) = 0 \tag{4.9}$$

lying in the upper half of the k-plane, and although it is not possible to solve (4.9) analytically, it can be shown numerically that there is in fact just a single root in the upper half-plane, at $k = \kappa$ say. The numerical technique employed in calculating κ was suggested by Brazier-Smith & Scott (1991), and involves the use of winding-number integrals (a brief description of its application to our problem is given in Appendix B); this approach proves particularly efficient since it does not involve the numerical solution of the linearized lower-deck equations. Some simplification of (4.9) is possible when S is either large or small, and it can be shown that

$$\kappa \sim S^{\frac{1}{2}} \exp(3\pi \mathrm{i}/4) \quad \text{as} \quad S \to \infty \ , \tag{4.10}$$

as found by Daniels (1975), whilst

$$\kappa \sim \mathrm{i}\left[-3\mathrm{Ai}'(0)\right]^{\frac{3}{4}} \quad \text{as} \quad S \to 0 \ , \tag{4.11}$$

corresponding to the Stewartson & Williams (1969) steady eigensolution. The path of the single zero in the k-plane for varying S was calculated using our winding-number technique, and was seen to be in agreement with both these limits; this path is shown in figure 6, Appendix B.

Once the single root $k = \kappa$ of (4.9) has been determined numerically for a given value of S, the unsteady displacement can be written down in the form

$$\bar{A}(X) = \mathrm{i}\frac{E_2'}{\kappa} \exp(-\mathrm{i}\kappa X) \quad \text{for} \quad X < 0 \, , \tag{4.12}$$

$$\bar{A}(X) = E_2'(X + \mathrm{i}/\kappa) \quad \text{for} \quad X > 0 \ . \tag{4.13}$$

Here we have used the fact that, in order for the pressure to be continuous in the lower deck, $\bar{A}(X)$ must be smooth for all X (and in particular for $X = 0$), and this has been achieved by fixing the values of both the arbitrary constant D of (3.11) and of a second arbitrary constant corresponding to the coefficient of $\bar{A}(X)$ in $X < 0$. The longitudinal unsteady velocity above the plate in $X < 0$ is

$$\bar{U}(X, Y) = \mathrm{i}\kappa E_2' \mathscr{K}(\kappa, Y) \exp(-\mathrm{i}\kappa X) \ , \tag{4.14}$$

and we write the corresponding unsteady streamfunction as $\bar{\psi}(X, Y)\exp(\mathrm{i}T)$, and for definiteness fix $\bar{\psi}(X, 0) = 0$. Below the plate it can be shown that $U(X, Y) = 0$ for $X \leqslant 0$, as in the unsteady lower-deck solution of the subsonic splitter-plate problem (Daniels 1978).

4.2. *Unsteady flow downstream of the trailing edge*

We have therefore determined analytically the unsteady velocity in the lower deck upstream of the trailing edge, and in particular at $X = -0$, and we now go on to calculate the evolution of this trailing-edge velocity profile downstream. The steady flow in $X > 0$ is just the inner limit of the steady Goldstein wake (Stewartson 1969); it can easily be shown that for $X > 0$ the streamfunction, $\psi_s(X, Y)$, associated with the steady flow is

$$\psi_s(X, Y) = \xi^2 f_0(\eta) \ , \tag{4.15}$$

where $\xi = X^{\frac{1}{3}}$ and $\eta = Y/\xi$, and where

$$f_0''' = (f_0'^2 - 2f_0 f_0'')/3 \tag{4.16}$$

subject to $f_0'(\eta) \sim 0$ as $\eta \to -\infty$ and $f_0(\eta) \sim \eta^2/2$ as $\eta \to \infty$. The unsteady lower-deck equations are again linearized by treating the amplitude of the unsteady flow as

being much smaller than that of the steady flow, and the resulting system solved numerically; we note that, owing to the abrupt change in boundary conditions at the trailing edge, the two-region scheme first developed by Smith (1974), and later applied to a number of different wake flows by Daniels (1976), must be used. We define region I, in which $\eta = O(1)$ and in which the steady base flow is given by (4.15), and region II, in which η is large and in which the steady flow is simply uniform shear, and perform the linearization in each region separately. In region I, the streamfunction associated with the total flow is written as $\xi^2 G(\xi, \eta, T)$, and in order to linearize about the steady base flow we define the streamfunction associated with the small unsteady part of the flow as $\xi^2 \bar{G}(\xi, \eta) \exp(\mathrm{i}T)$, with

$$G(\xi, \eta, T) = f_0(\eta) + \bar{G}(\xi, \eta) \exp(\mathrm{i}T) \ . \tag{4.17}$$

After substitution into (3.2) and neglect of quadratic terms we arrive at the linearized equation governing the downstream evolution of $\bar{G}$ in the form

$$\mathrm{i}S\xi \frac{\partial \bar{G}}{\partial \eta} + \frac{1}{3}\left\{ f_0' \frac{\partial^2 \bar{G}}{\partial \xi \partial \eta} - f_0'' \frac{\partial \bar{G}}{\partial \xi} \right\} = \frac{1}{\xi} \frac{\partial^3 \bar{G}}{\partial \eta^3} - \frac{2f_0'}{3\xi} \frac{\partial \bar{G}}{\partial \eta} + \frac{2f_0}{3\xi} \frac{\partial^2 \bar{G}}{\partial \eta^2} + \frac{2f_0'' \bar{G}}{3\xi} \ . \tag{4.18}$$

In region II, the streamfunction associated with the total flow is denoted $F(\xi, Y, T)$, and we write

$$F(\xi, Y, T) = \tfrac{1}{2} Y^2 + \bar{F}(\xi, Y) \exp(\mathrm{i}T) \ ; \tag{4.19}$$

proceeding as before, it can be shown that $\bar{F}$ satisfies

$$\mathrm{i}S\xi^2 \frac{\partial \bar{F}}{\partial Y} + \frac{Y}{3} \frac{\partial^2 \bar{F}}{\partial Y \partial \xi} - \frac{1}{3} \frac{\partial \bar{F}}{\partial \xi} = \xi^2 \frac{\partial^3 \bar{F}}{\partial Y^3} \ . \tag{4.20}$$

The problem of determining the unsteady velocity field in $X > 0$ is parabolic in X, and we therefore need to specify the initial profile in both regions I and II at $X = 0$. The unsteady streamfunction and its Y-derivatives on $X = 0$ in region II have already been calculated analytically in the previous section. Turning to region I, in order to specify the initial condition for the streamwise marching at $\xi = 0$, the limiting behaviour of $\bar{G}(\xi, \eta)$ as $\xi \to +0$ must first be determined, and to obtain this we note that the unsteady shear stress on the plate at the trailing edge is $\bar{\lambda} \exp(\mathrm{i}T)$, where from (4.14)

$$\bar{\lambda} = \frac{\mathrm{i}\kappa E_2' \mathrm{Ai}(y_0)}{[(\kappa + \mathrm{i}\delta) \exp(-\mathrm{i}\pi/2)]^{\frac{1}{3}} \mathrm{Ai}'(y_0)} \ , \tag{4.21}$$

so that the total effective shear stress at the base of region II for $X = +0$ is $1 + \bar{\lambda} \exp(\mathrm{i}T)$. The streamfunction in region I which matches onto this outer flow in region II is then simply obtained by rescaling the steady streamfunction described in (4.16), and it follows that

$$G(\xi, \eta, T) \sim [1 + \bar{\lambda} \exp(\mathrm{i}T)]^{\frac{1}{3}} f_0([1 + \bar{\lambda} \exp(\mathrm{i}T)]^{\frac{1}{3}} \eta) \quad \text{as} \quad \xi \to +0 \ . \tag{4.22}$$

Finally, equation (4.22) is linearized by setting $\bar{\lambda} \ll 1$, and by comparison with (4.17) we see that

$$\bar{G}(\xi, \eta) = \tfrac{1}{3} \bar{\lambda} (f_0(\eta) + \eta f_0'(\eta)) \quad \text{as} \quad \xi \to +0 \ , \tag{4.23}$$

thereby specifying the flow in the inner region near the trailing edge.

Full details of the numerical procedure are given by Smith (1974), and we merely note here that the equations (4.18) and (4.20) are discretized using a central difference scheme, and that the mesh points in region I are chosen to be uniformly spaced in ξ and η, whilst in region II they are uniformly spaced in ξ and Y. The unsteady

streamfunction and its first two Y-derivatives are matched on the boundary between the two regions, whilst boundary condition (4.5) is applied on the upper edge of region II and the unsteady velocity is set to zero on the lower edge of region I. The resulting matrix equation, expressing the flow at a given ξ-station in terms of the flow at the previous upstream station, can then easily be solved by pivoting and back substitution; the solution is started with the asymptotic result for the unsteady flow very close to the trailing edge, as described above, and then marched downstream. At $\xi = 1$ regions I and II are replaced by a single uniform grid of equally spaced X and Y points.

4.3. *Asymptotic solution downstream*

Following Daniels (1975) we make the substitutions $\tilde{Y} = Y - A$ and $\tilde{V} = V - S\partial A/\partial T - U\partial A/\partial X$ in the full nonlinear lower-deck equation (3.3) and its boundary conditions, and whilst (3.3) remains unchanged, boundary condition (3.8) becomes simply $U \to \tilde{Y}$ as $\tilde{Y} \to \infty$; it is then clear that a solution for U is of the form

$$U = \xi f_0'(\tilde{\eta}) \ , \tag{4.24}$$

where $\tilde{\eta} = \tilde{Y}/\xi$. We note here that this solution satisfies the nonlinear lower-deck equation and the boundary conditions at $\tilde{Y} = \pm\infty$ exactly for all X, but clearly does not match at $X = 0$ with the flow upstream of the trailing edge. We would therefore expect the lower-deck velocity to evolve downstream from the trailing edge so as to approach the flow described by (4.24), and this indeed turns out to be the case. The implication of equation (4.24) is that the nonlinear unsteady flow evolves downstream into the form of a steady wake flow which has its centreline aligned along the line $Y = A(X, T)$, and from (3.11) it follows that this centreline is a straight line whose gradient oscillates harmonically in time with amplitude E_2'. In terms of the outer variables, the equation of the wake centreline as $X \to \infty$ is therefore

$$y = (M^2 - 1)^{\frac{1}{2}} E_2 x \exp(\mathrm{i}\omega t)/p_\infty \ , \tag{4.25}$$

and we see that this is identical to the equation for the vortex-sheet deflection as $x \to 0$ given in equation (2.12). We can therefore conclude that the flow described by equation (4.24) matches with the outer solution downstream of the trailing edge, and all that remains to be verified is that the lower-deck flow does indeed converge onto (4.24) as $X \to \infty$.

In order to make a consistent comparison between the numerical linearized lower-deck solution and (4.24), we need to linearize (4.24) as before, and using our expression for $A(X, T)$ in $X > 0$ it can be seen that the streamfunction associated with (4.24) approaches

$$(E_2')(X + \mathrm{i}/\kappa)\xi f_0'(\eta) \quad \text{as} \quad \xi \to \infty \ . \tag{4.26}$$

This can then be compared with the computed values for $\xi^2 \bar{G}(\xi, \eta)$.

4.4. *Numerical results*

The linearized equations in the lower deck downstream of the trailing edge were integrated numerically as described above. The step size in the streamwise direction was taken as 0.05 for ξ both less than and greater than 1, and the equations were integrated as far as $X = 5$, with the solution compared to the downstream asymptotic solution at each step. It was found that a step size of 0.1 in both η and Y was perfectly adequate, whilst the boundary conditions at infinity could be applied on $\eta = -10$ and $Y = 6$.

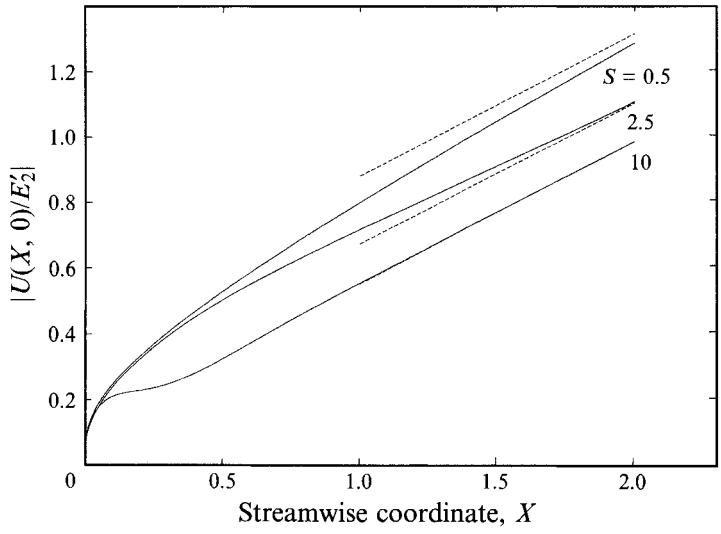

FIGURE 4. The computed amplitude of the normalized longitudinal velocity component in the lower deck on the centreline, $|U(X,0)/E_2'|$, plotted against streamwise coordinate X downstream of the trailing edge for $S = 0.5, 2.5$, and 10 (solid lines), together with the corresponding asymptotic downstream solution (dashed lines).

The computed values of $|U(X,0)/E_2'|$ are plotted in figure 4 for various values of the frequency parameter S, and are compared with the asymptotic solution described in the previous subsection (it is easy to show that the parameter E_2' is independent of frequency for $\omega = O(\epsilon^{-2})$, and hence independent of S, when the amplitude of the acoustic pressure forcing the motion is held fixed, so that the flows described in figure 4 are forced by acoustic waves of differing frequencies but of the same pressure). In the vicinity of the trailing edge the unsteady flow close to $Y = 0$ is driven by the unsteady shear stress, $\bar{\lambda}$, at the trailing edge, and the flow for each S corresponds to the limiting form given in (4.22), with the unsteady velocity proportional to $X^{\frac{1}{3}}$ as $X \to +0$. In contrast, sufficiently far downstream the flow is essentially determined by the local value of the unsteady displacement thickness, $A(X)$, and we have $A(X) \propto X + \mathrm{i}/\kappa$, so that the velocity grows linearly downstream. These two regions of X small and X large are joined smoothly over intermediate values of X, for which no asymptotic solution is available. For each value of S considered, the computed unsteady velocity converges to the asymptotic solution given in (4.24) downstream, confirming that the downstream behaviour of the lower-deck flow is fully consistent with the potential-theory solution in the outer flow. As might be expected, since $1/S$ is essentially a measure of the lengthscale of the unsteady flow, the distance downstream taken to converge to the asymptotic solution is seen to decrease as S increases; indeed, when S is as large as 10, the computed and asymptotic solutions are indistinguishable for $X > 1$. In addition, the magnitude of the unsteady velocity appears to be relatively insensitive to S close to the trailing edge but decreases with increasing S further downstream, and this can be understood by considering the limit $S \to \infty$. It can easily be shown from (4.18) that for large values of S the expression for the unsteady flow near the trailing edge given in (4.22) is valid for $X < O(S^{-\frac{3}{2}})$, so that in this region the flow is driven by the value of $\bar{\lambda}$, and it turns out that $\bar{\lambda}$ converges to its (finite and non-zero) large-S limit very quickly as S is increased, and is virtually independent of S for $S = O(1)$. For $X > O(S^{-\frac{3}{2}})$ it can be seen from (4.26) that

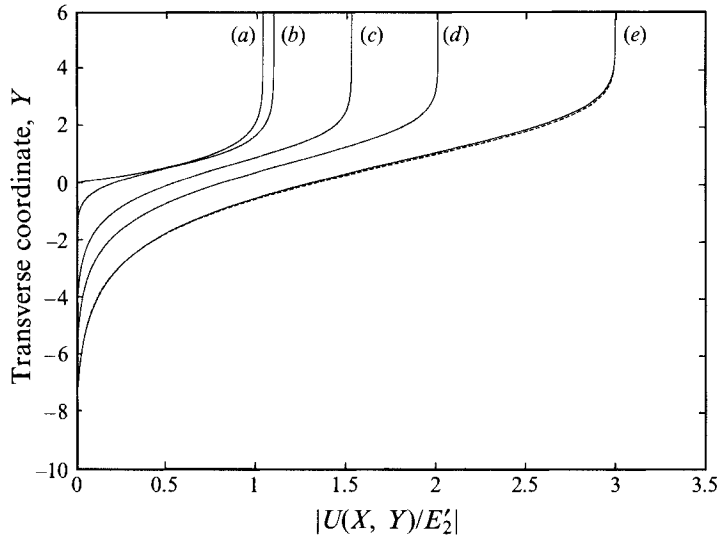

FIGURE 5. The computed amplitude of the normalized longitudinal velocity component in the lower deck (solid lines), $|U(X,Y)/E_2'|$, plotted against transverse coordinate Y, for various values of downstream coordinate X: (*a*) $X = 0.02$; (*b*) $X = 0.4$; (*c*) $X = 0.8$; (*d*) $X = 1$; (*e*) $X = 2$. The downstream asymptotic solution is plotted at $X = 2$ (dashed line).

the quantity $|U(X,Y)/E_2'|$ approaches the non-zero limit $f_0''(\eta)X$ monotonically as $S \to \infty$.

In figure 5 we plot the downstream evolution of the unsteady longitudinal velocity profile $|U(X,Y)/E_2'|$ for the particular value $S = 0.5$; we merely note here that the transverse extent of the layer over which the unsteady flow adjusts from its zero value as $Y \to -\infty$ to the value $-A(X)$ as $Y \to \infty$ increases rapidly downstream, with width proportional to $X^{\frac{1}{3}}$. The computed profile at $X = 2$ is seen to be in very close agreement with the downstream asymptotic solution.

5. Concluding remarks

We have therefore seen that the single plausible outer potential-theory solution to our supersonic splitter-plate problem, in which the unsteady pressure is discontinuous and the vortex sheet has non-zero gradient at the trailing edge, can be matched consistently with the inner viscous flow near the trailing edge for the choice of frequency $\omega = O(\epsilon^{-2})$ and incident amplitude $I = O(\epsilon^4)$. Very close to the trailing edge in the lower deck the dividing streamline in our unsteady flow can be shown to oscillate harmonically about the location of the steady dividing streamline, $Y = 0.895X^{\frac{1}{3}}$, with an amplitude proportional to the unsteady shear stress $\bar{\lambda}$, and since in our linearized flow $\bar{\lambda}$ is small the dividing streamline at the trailing edge is seen to bend up into the moving fluid at all times. This is exactly the same behaviour as encountered in the full-Kutta-condition solution of the subsonic splitter-plate problem (Daniels 1978), the only difference here being the functional form of the unsteady shear stress. Further downstream, however, the equation of the dividing streamline will be

$$Y = 0.895X^{\frac{1}{3}} + E_2'X\exp(\mathrm{i}T) \quad \text{as} \quad X \to \infty\ , \tag{5.1}$$

so that even when the unsteady flow is only a weak perturbation to the steady base flow (i.e. $|E_2'| \ll 1$) the dividing streamline will oscillate about $Y = 0$ for sufficiently

large X, and this exactly matches with the behaviour of the vortex sheet in the outer flow near the trailing edge. In addition, by considering the deflection of the vortex sheet at the trailing edge, it is seen that significant unsteady shear-layer disturbances can be generated at the trailing edge by acoustic waves propagating from upstream over a wide range of acute values of the incidence angle, and this seems particularly significant, since it suggests that noise generated by engine components well upstream of the nozzle can have a marked effect on the unsteady behaviour of the jet near the nozzle.

With regard to the question of flow separation, in the linearized analysis of § 4 we assumed that $\bar{\lambda} \ll 1$, so that separation cannot occur; when $\bar{\lambda} = O(1)$, however, an exact separation condition could only be determined via a numerical solution of the full unsteady nonlinear lower-deck equations, and that has not been attempted. Our results can be used to determine an approximate separation condition, however; the condition $\bar{\lambda} \ll 1$ is equivalent to $|E_2'| \ll 1$, and by writing $I = \epsilon^4 \tilde{I}$ it is easy to see that

$$|E_2'| \propto (M_\infty^2 - 1)^{\frac{1}{4}} |\tilde{I}| D(\theta_i) \exp(-\Lambda(k_1)) \ , \tag{5.2}$$

where $D(\theta_i)$ is a complicated function of incidence angle, θ_i, and $\Lambda(k_1)$ is defined in Appendix A. For $\theta_i < \pi/2$, $D(\theta_i)$ is $O(1)$, and it therefore follows that for $\omega = O(\epsilon^{-2})$ our unsteady flow will not separate from the trailing edge provided that

$$(M_\infty^2 - 1)^{\frac{1}{4}} |\tilde{I}| \exp(-\Lambda(k_1)) \tag{5.3}$$

is significantly smaller than unity. For forcing at a lower frequency (i.e. when $\omega = o(\epsilon^{-2})$), then provided that I is chosen such that the pressure at the trailing edge remains $O(\epsilon^2)$, the problem in the lower deck would reduce to a form exactly equivalent to that found for a plate inclined into a steady supersonic stream on one side with zero flow on the other side, and a separation condition derived in exactly the same way as described by Daniels (1975) for an oscillating airfoil in supersonic flow.

Finally, we remark that our unique solution of the *supersonic* splitter-plate problem will be of relevance to further investigations into the question of exactly which of the non-unique outer solutions of the *subsonic* splitter-plate problem is realized in practice. We proceed by attempting to determine the transonic limit of our supersonic solution (i.e. taking the limit $M \to 1$ in the results presented here), and then comparing this with the limiting behaviour of the various subsonic solutions. As a preliminary result, we note that from equation (2.12) the coefficient of the first term in the expansion of the vortex-sheet deflection as $x \to +0$ is identically zero for $M = 1$, so that the vortex-sheet deflection is no longer proportional to x; it turns out, by setting $M = 1$ in the outer potential-theory problem, that $\eta(x) \propto x^{\frac{3}{2}}$ as $x \to +0$, which is in fact reminiscent of the vortex-sheet behaviour of the full-Kutta-condition solution in subsonic flow. However, analysis of both the inner and outer unsteady flow regimes will be required in order to resolve this question satisfactorily, involving the transonic triple-deck scalings first identified by Messiter, Feo & Melnik (1971), and work is now well under way in this direction.

The author is very grateful to Professor D.G. Crighton for suggesting this problem and to Professor P.G. Daniels for a number of helpful conversations, and is pleased to acknowledge the financial support of the Royal Society.

Appendix A

In this appendix we state the decomposition of the Wiener–Hopf kernel function $G(k)$ for the outer potential problem of § 2 – see Morgan (1974) for full details. We define $\Gamma(k)$ by

$$G(k) = \frac{(k-u_0)(k-u_0^*)}{\gamma_1(k)\gamma_2(k)}\Gamma(k) \ , \tag{A 1}$$

where

$$\Gamma(k) \equiv \frac{\gamma_1(k)k_0^2 + \gamma_2(k)(k_0 - Mk)^2}{(k-u_0)(k-u_0^*)} \ , \tag{A 2}$$

and where u_0 and u_0^* are the zeros of $G(k)$, and it is therefore clear that $\Gamma(k)$ is non-zero throughout the complex k-plane. $\Gamma(k)$ can now be factorized in the form $\Gamma(k) = \Gamma^+(k)\Gamma^-(k)$, with $\Gamma^\pm(k)$ analytic and non-zero in the half-planes $R^\pm$ respectively, using the Cauchy-integral formulation described by Noble (1958); for instance, for k lying in the strip $R^+ \cap R^-$, we have

$$\log \Gamma^-(k) = -\frac{1}{2\pi i}\int \frac{\log \Gamma(z)}{z-k}\mathrm{d}z \ , \tag{A 3}$$

where the integration contour lies within the strip but passes above the point $z = k$. This integral can be considerably simplified (Morgan 1974); we proceed by deforming the contour to lie around the branch cut in the upper half-z-plane, yielding contributions from the branch-cut integral and from the circle at infinity, and it can be shown that

$$\Gamma^-(k) = \gamma_2^-(k)\exp(\Lambda(k)) \ , \tag{A 4}$$

where

$$\Lambda(k) = -\frac{1}{\pi}\int_{-k_0}^{-\infty} \frac{\left\{\tan^{-1}\left[|\gamma_2(z)|/|\gamma_1(z)|\left(1 - Mz/k_0\right)^2\right] - \pi/2\right\}}{z-k}\mathrm{d}z \ . \tag{A 5}$$

Hence, using the fact that $\gamma_1^-(k) = 1$, we see that

$$G^-(k) = \exp(\Lambda(k)) \ , \tag{A 6}$$

$$G^+(k) = \frac{(k-u_0)(k-u_0^*)}{\gamma_1(k)\gamma_2(k)}\Gamma(k)\exp(-\Lambda(k)) \ . \tag{A 7}$$

It can easily be seen that $G^-(k)$ is analytic and non-zero in R^-, and that $G^-(k) \sim 1$ as $k \to \infty \in R^-$. The analyticity of $G^+(k)$ in R^+ is guaranteed by the fact that $\gamma_1(k)$ is analytic throughout R^+, and by the fact that $\Lambda(k)$ is logarithmically divergent at $k = -k_0$ (so that $G^+(k)$ is regular in the neighbourhood of the branch point in the upper half-plane at $k = -k_0$). It follows that

$$G^+(k) \sim -M^2k/(M^2-1)^{\frac{1}{2}} \tag{A 8}$$

as $k \to \infty \in R^+$.

Appendix B

In this appendix we briefly describe the use of the winding-number integral and its first moment to determine the root of the equation

$$\mathscr{K}(k,0) = 0 \tag{B 1}$$

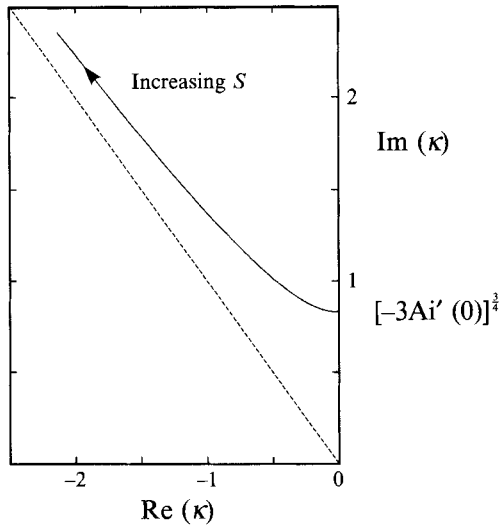

FIGURE 6. The path of the single zero, κ, of equation (4.9) lying in the upper half-plane as S is increased from zero to a maximum value of 10 (solid line), with the asymptotic limit as $S \to \infty$ (dashed line).

in the upper half of the complex k-plane; full details of this method are given by Brazier-Smith & Scott (1991). The generalized winding-number integral for any function $F(k)$ around a given closed curve in the complex plane is

$$I_m = \frac{1}{2\pi \mathrm{i}} \oint k^m \frac{F'(k)}{F(k)} \mathrm{d}k \ , \tag{B 2}$$

where $'$ denotes differentiation with respect to k, and it is well-known that $I_0 = n_z - n_p$, where $n_{z,p}$ are the numbers of zeros and poles of $F(k)$ enclosed within the integration contour. In our problem, it will be more convenient to consider $\mathscr{J}(k,0) \equiv k^2 \mathscr{K}(k,0)$ instead of $\mathscr{K}(k,0)$, since $\mathscr{J}(k,0)$ possesses no poles in the upper half-plane and since $\mathscr{J}(k,0) \propto k^{\frac{4}{3}}$ as $k \to \infty$, so that there are no zeros of $\mathscr{J}(k,0)$ far from the origin. We note further that the corresponding expression for I_0 can be integrated once to give

$$I_0 = \frac{1}{2\pi \mathrm{i}} [\log \mathscr{J}(k,0)] \ , \tag{B 3}$$

where the square brackets denote the change in $\log \mathscr{J}(k,0)$ in going once round the closed contour, and the definition of the complex logarithm is the standard one in which the branch cut lies along the negative real axis.

We therefore proceed by choosing integration contours lying in the upper half-plane and calculating the variation of $\log \mathscr{J}(k,0)$ round each contour; obviously, I_0 changes by 1 each time the value of $\mathscr{J}(k,0)$ crosses the negative real axis. In this way, by choosing rectangular contours so as to cover all of the upper half-plane in which $k = O(1)$, it is possible to demonstrate that $\mathscr{J}(k,0)$ has only one zero in the upper half-plane, and that this zero lies in the second quadrant. In order to determine the position of this single zero, we proceed as in Brazier-Smith & Scott (1991), and calculate the first moment of the winding integral for $\mathscr{J}(k,0)$, which can be simplified as

$$I_1 = \frac{1}{2\pi \mathrm{i}} [z \log \mathscr{J}(k,0)] - \frac{1}{2\pi \mathrm{i}} \oint \log \mathscr{J}(k,0) \mathrm{d}k \ . \tag{B 4}$$

In our case, since $\mathscr{J}(k,0)$ possesses only a single zero, at $k = \kappa$ say, it can easily be shown that $I_1 = \kappa$.

This method is therefore particularly efficient in our problem, since we have demonstrated that there is only a single root of (B 1) in the upper half-plane simply by evaluating $\log \mathscr{J}(k,0)$ at several points round suitably chosen closed curves, whilst the position of this zero has been determined with the need to evaluate only a single integral (i.e. the integral of $\log \mathscr{J}(k,0)$) numerically. The numerical integration was performed using the simple trapezium rule, and was seen to be accurate even when only a relatively small number of subintervals round the contour were used. This approach appears to be more efficient than alternative techniques for determining κ, such as numerical solution of the linearized lower-deck differential equation, or solution of (B 1) by Newton–Raphson iteration. The path of the single zero in the upper half of the k-plane as S is increased from zero is shown in figure 6.

REFERENCES

BRAZIER-SMITH, P. R. & SCOTT, J. F. M. 1991 On the determination of the roots of dispersion equations by use of winding number integrals. *J. Sound Vib.* **145**, 503–510

BROWN, S. N. & DANIELS, P. G. 1975 On the viscous flow about the trailing edge of a rapidly oscillating plate. *J. Fluid Mech.* **67**, 743–761.

BROWN, S. N. & STEWARTSON, K. 1970 Trailing-edge stall. *J. Fluid Mech.* **42**, 561–584.

CARGILL, A. M. 1982 Low-frequency sound radiation and generation due to the interaction of unsteady flow with a jet pipe. *J. Fluid Mech.* **121**, 59–105.

CRIGHTON, D. G. 1972*a* Radiation properties of the semi-infinite vortex sheet. *Proc. R. Soc. Lond.* A**330**, 185–198.

CRIGHTON, D. G. 1972*b* Radiation properties of the semi-infinite vortex sheet. In *Papers on Novel Aerodynamic Noise Source Mechanisms at Low Speeds*. Ministry of Defence (Procurement Executive) CP 1195.

CRIGHTON, D. G. 1985 The Kutta condition in unsteady flow. *Ann. Rev. Fluid Mech.* **17**, 411–445.

CRIGHTON, D. G. & LEPPINGTON, F. G. 1974 Radiation properties of the semi-infinite vortex sheet: the initial-value problem. *J. Fluid Mech.* **64**, 393–414.

DANIELS, P. G. 1974 Numerical and asymptotic solutions for the supersonic flow near the trailing edge of a flat plate. *Q. J. Mech. Appl. Maths* **27**, 175–191.

DANIELS, P. G. 1975 The flow about the trailing edge of a supersonic oscillating aerofoil. *J. Fluid Mech.* **72**, 541–557.

DANIELS, P. G. 1976 A numerical and asymptotic investigation of boundary-layer wake evolution. *J. Inst. Maths Applics.* **17**, 367–386.

DANIELS, P. G. 1977 Viscous mixing at a trailing edge. *Q. J. Mech. Appl. Maths* **30**, 319–342.

DANIELS, P. G. 1978 On the unsteady Kutta condition. *Q. J. Mech. Appl. Maths* **31**, 49–75.

GUO, Y. P. 1990*a* Sound generation by a supersonic aerofoil cutting through a steady jet flow. *J. Fluid Mech.* **216**, 193–212.

GUO, Y. P. 1990*b* Sound radiation from sources near a sharp trailing edge in a supersonic mean flow. *AIAA Paper* 90-3913.

HOWE, M. S. 1978 A review of the theory of trailing edge noise. *J. Sound Vib.* **61**, 437-465.

JONES, D. S. 1972 Aerodynamic sound due to a source near a half-plane. *J. Inst. Maths Applics* **9**, 114–122.

JONES, D. S. & MORGAN, J. D. 1972 The instability of a vortex sheet on a subsonic stream under acoustic radiation. *Proc. Camb. Phil. Soc.* **72**, 465–488.

JONES, D. S. & MORGAN, J. D. 1973 The instability due to acoustic radiation striking a vortex sheet on a supersonic stream. *Proc. R.S.E.* **71**, 121–140.

MESSITER, A. F. 1970 Boundary-layer flow near the trailing edge of a flat plate. *SIAM J. Appl. Maths* **18**, 241–257.

MESSITER, A. F., FEO, A. & MELNIK, R. E. 1971 Shock-wave strength for separation of a laminar boundary layer at transonic speeds. *AIAA J.* **9**, 1197–1198.

MORGAN, J. D. 1974 The interaction of sound with a semi-infinite vortex sheet. *Q. J. Mech. Appl. Maths* **27**, 465–487.

NOBLE, B. 1958 *Methods Based on the Wiener-Hopf Technique*. Pergamon.

ORSZAG, S. A. & CROW, S. C. 1970 Instability of a vortex sheet leaving a semi-infinite plate. *Stud. Appl. Maths* **49**, 167–181

RIENSTRA, S. W. 1981 Sound diffraction at a trailing edge. *J. Fluid Mech.* **108**, 443–460.

SMITH, F. T. 1974 Boundary layer flow near a discontinuity in wall conditions. *J. Inst. Maths Applics* **13**, 127–145.

STEWARTSON, K. 1964 *The Theory of Laminar Boundary Layers in Compressible Fluids*. Oxford University Press.

STEWARTSON, K. 1969 On the flow near the trailing edge of a flat plate II. *Mathematika* **16**, 106–121.

STEWARTSON, K. & WILLIAMS, P. G. 1969 Self-induced separation. *Proc. R. Soc. Lond.* A**312**, 181–206.